

The effect of Dark Matter and Dark Energy interactions on the peculiar velocity field and the kinetic Sunyaev-Zel'dovich effect

Xiao-Dong Xu, Bin Wang, Pengjie Zhang

*Department of Physics and Astronomy,
Shanghai Jiao Tong University, Shanghai 200240, China*

Fernando Atrio-Barandela

Departamento de Física Fundamental, Universidad de Salamanca, Spain

Abstract

The interaction between Dark Matter and Dark Energy has been proposed as a mechanism to alleviate the coincidence problem. We analyze its effects on the evolution of the gravitational and the peculiar velocity fields. We find that for different model parameters peculiar velocities vary from a factor five times smaller to two times larger than in the Λ CDM cosmological model at the same scales. We propose two new observables sensitive to such interactions based on their effect on the velocity field. We compare the effects on peculiar velocities with those on the Integrated Sachs-Wolfe effect demonstrating that velocities are more sensitive to the interaction. We show that the current upper limits on the amplitude of the kinetic Sunyaev-Zel'dovich power spectrum of temperature anisotropies provide constraints on the coupling within the dark sectors that are consistent with those obtained previously from the Cosmic Microwave Background and galaxy clusters. In particular, we show that Atacama Cosmology Telescope and South Pole Telescope data favor the decay of Dark Energy into Dark Matter, as required to solve the coincidence problem.

PACS numbers: 98.80.Es, 98.80.Bp, 98.80.Jk

I. INTRODUCTION

Luminosity distances derived from Type-Ia supernovae (SNIa) were the first cosmological observations to establish that today the expansion of the Universe is being accelerated [1–7], driven by a so-called dark energy (DE) with equation of state (EoS) parameter $w \approx -1$. Observations of the temperature anisotropies of the Cosmic Microwave Background (CMB) indicated that the dominant energy component, with $\sim 70\%$ of the total energy density is DE, $\sim 26\%$ cold dark matter (DM) and a small fraction (4%) of baryonic matter [8, 9]. The nature of both DM and DE are unknown. They couple to baryons and radiation only through gravity but in the context of field theory other interactions within the dark sector can also exist [10, 11]. A DM-DE interaction provides a natural way to alleviate the coincidence problem, which embarrasses the standard Λ CDM cosmology [12–18]. Also, the appropriate interaction can accommodate an effective DE EoS with $w < -1$ at the present time [19, 20]. A non-gravitational coupling in the dark sector will affect significantly the expansion history of the Universe and the evolution of density perturbations, changing their growth. The possibility of the DE-DM interaction has been widely discussed in the literature [12–18, 21–46]. Thus, determining the existence of DM-DE interactions is an observational endeavour that could provide an interesting insight into the nature of the dark sector.

Several authors have looked for observational signatures of the interaction using Wilkinson Microwave Anisotropy Probe (*WMAP*), SNIa and Baryon Oscillation Observation (BAO) data [30–37] together with complementary probes on the growth of cosmic structures [40–47]. Until now the data have provided only upper limits on the amplitude of the interaction, requiring the strength of the coupling to be $\leq 10^{-3}$ [45, 48–50]. Therefore, it is necessary to search for more sensitive probes. For instance, the interaction changes the time evolution of the gravitational potential [36, 47] and leaves a signature in the late Integrated Sachs-Wolfe (ISW) effect [36, 48, 51]. Due to cosmic variance, the statistical power of the late-time ISW to constrain DM-DE interactions is limited. Nevertheless, since the coupling between the dark sectors also influences the absolute value of the gravitational potential and changes the peculiar motion of the different matter particles, it provides two new observational tests. First, matter peculiar velocities can be measured using galaxy surveys and kinetic Sunyaev-Zel’dovich (kSZ) temperature anisotropies. Depending on model parameters, the interaction changes the amplitude of matter peculiar velocities by a factor two to five with

respect to the fiducial Λ CDM model. While these variations are significant, they are still within the upper limit set by *Planck* [52]. Second, the diffuse intergalactic medium and the unresolved cluster population generate temperature anisotropies on the CMB at small scale via the conventional kSZ effect and any change of the baryon peculiar velocity field will also change the power spectrum of the kSZ anisotropies. In this paper we will show that both observational tests are potentially powerful probes of DM-DE interactions.

In general, the kSZ effect is sensitive to the dynamical evolution of matter in the Universe. Large scale bulk flows and the mean pairwise velocity dispersion of clusters have already been reported [53–57]. The kSZ effect is also a potential probe of reionization, the radial inhomogeneities in the Lemaître-Tolman-Bondi [58], the missing baryon problem [59], the dark flow [60], etc. Throughout the paper we will consider only a flat cosmological model with the following cosmological parameters: Hubble constant $H_0 = 67.11 \text{ km s}^{-1} \text{ Mpc}^{-1}$, baryon abundance $\Omega_b h^2 = 0.0221$, DE fraction $\Omega_d = 0.68$ (for Λ CDM model, $\Omega_\Lambda = 0.68$), scalar spectral index $n_s = 0.9624$ and amplitude of primordial curvature perturbation $10^9 A_s = 2.215$. Briefly, in Sec. 2 we will introduce the equations describing the evolution of DM and DE density perturbations. In Sec. 3, we will study the effect of the interaction on the evolution of the gravitational field and its contribution to the Integrated Sachs Wolfe effect. In Sec. 4, we will analyze the effect on peculiar velocities and in Sec. 5 we will compute the power spectrum of the CMB temperature anisotropies generated by the kSZ effect. Finally, in Sec. 6 we will summarize our main results and present our conclusions.

II. THE MODEL OF THE INTERACTION BETWEEN DE AND DM

The formalism describing the evolution of matter and DE density perturbations without [61, 62] and with DM-DE interaction [40] is well established. If DM and DE are coupled with each other, the energy-momentum tensor $T_\lambda^{\mu\nu}$ of each individual component $\lambda = (c, d)$ is no longer conserved. Instead,

$$\nabla_\mu T_\lambda^{\mu\nu} = Q_\lambda^\nu, \quad (1)$$

where Q_λ^ν is the four vector governing the energy-momentum transfer between dark components and the subscripts c, d refer to DM and DE, respectively. Since DM and DE couple to all other energy densities in the Universe only through gravity, the energy-momentum tensor of DM+DE is conserved, i.e., $\sum_\lambda \nabla_\mu T_\lambda^{\mu\nu} = 0$. Then, $Q_c^\nu = -Q_d^\nu$.

Assuming spatially flat Friedmann-Robertson-Walker background, from eq (1) we can derive the equations of evolution of the mean DM and DE densities

$$\dot{\rho}_c + 3H\rho_c = Q_c, \quad \dot{\rho}_d + 3H(1+w)\rho_d = Q_d, \quad (2)$$

where $Q_\lambda = aQ'_\lambda$ indicates the energy transfer, Q'_λ is the time component of the four vector Q'_λ and a the scale factor. Dots represent derivatives with respect to the coordinate time. Since the physical properties of DM and DE at the present moment are unknown, we cannot derive the precise form of the interaction from first principles. For simplicity, we will consider a phenomenological description and thus write the interaction between DE and DM as a linear combination of energy densities of the dark sectors $Q_c = 3H(\xi_1\rho_c + \xi_2\rho_d)$ [24, 40]. With this functional form, ξ_1 and ξ_2 are dimensionless parameters. To simplify the problem, we will assume that these coefficients are independent of time and the EoS parameter w is constant.

If the interaction parameters are positive, the DE transfers energy to the DM while if they are negative, the transfer is in the opposite direction. While the sign of the interaction is unknown, thermodynamic considerations based on the second principle require the coupling constants to be positive [27]. Also, to avoid the unphysical solution of a negative dark energy density ($\rho_d < 0$) in the early Universe when $Q_c = 3H\xi_1\rho_c$ or $Q_c = 3H\xi(\rho_c + \rho_d)$ the couplings ξ_1, ξ must be positive [39]. In Fig. 1 we represent the ratio of the mean energy densities $r \equiv \rho_d/\rho_c$. In Fig. 1a we represent the ratio with $\xi_2 = 0$ and $\xi_1 = \xi_2$; in Fig. 1b we show $\xi_1 = 0$. There are two attractor solutions with $r = \text{const}$, in the past, if $\xi_1 > 0$, and in the future, if $\xi_2 > 0$ [13, 15, 21]. Compared with the Λ CDM model, positive couplings gives a slower evolution r , i.e., there exists a long period in the evolution of the Universe where the DM and DE densities are comparable, alleviating the coincidence problem.

We can further reduce the parameter space if we take into account that, at the background level and at first order in perturbation theory, models with $(\xi_1 = \xi_2 \neq 0)$ and $(\xi_1 \neq 0, \xi_2 = 0)$ show similar behavior. Also, since the fraction of DE at early times is small compared to the DM, models with interaction kernels $\xi_1 \neq \xi_2$ behave very similarly to models with $\xi_2 = 0$. If $Q_c = 3H\xi_1\rho_c$ or $Q_c = 3H\xi(\rho_c + \rho_d)$, curvature perturbations diverge if $w > -1$ so we restrict our study to $w < -1$. A discussion on the origin of this instability can be found in [24, 49]. If $Q_c = 3H\xi_2\rho_d$, there are no instabilities in the matter density perturbations, so we can consider EoS parameter with values larger and smaller than $w = -1$. To summarize, we

will study two interaction kernels: $Q_c = 3H\xi_1\rho_c$ and $Q_c = 3H\xi_2\rho_d$; in the first case, $\xi_1 > 0$ and $w < -1$; in the second, ξ_2 can have positive and negative value and w can be smaller or larger than -1. Other expressions, like the product of DM and DE densities, have also been discussed in the literature, but since they require a different treatment of first order perturbations we shall not consider them here.

The general gauge-invariant perturbation equations for DM and DE are [48]

$$D'_c = -kU_c + 3\mathcal{H}(\xi_1 + \xi_2/r)\Psi - 3(\xi_1 + \xi_2/r)\Phi' + 3\mathcal{H}\xi_2(D_d - D_c)/r, \quad (3)$$

$$U'_c = -\mathcal{H}U_c + k\Psi - 3\mathcal{H}(\xi_1 + \xi_2/r)U_c, \quad (4)$$

$$\begin{aligned} D'_d = & -3\mathcal{H}(C_e^2 - w)D_d + \{3w' + 9\mathcal{H}(C_e^2 - w)(\xi_1 r + \xi_2 + 1 + w)\}\Phi \\ & - 9\mathcal{H}^2(C_e^2 - C_a^2)\frac{U_d}{k} + 3(\xi_1 r + \xi_2)\Phi' - 3\mathcal{H}(\xi_1 r + \xi_2)\Psi \\ & + 3\mathcal{H}\xi_1 r(D_d - D_c) - 9\mathcal{H}^2(C_e^2 - C_a^2)(\xi_1 r + \xi_2)\frac{U_d}{(1+w)k} - kU_d, \end{aligned} \quad (5)$$

$$\begin{aligned} U'_d = & -\mathcal{H}(1 - 3w)U_d - 3kC_e^2(\xi_1 r + \xi_2 + 1 + w)\Phi + 3\mathcal{H}(C_e^2 - C_a^2)(\xi_1 r + \xi_2)\frac{U_d}{1+w} \\ & + 3\mathcal{H}(C_e^2 - C_a^2)U_d + kC_e^2 D_d + (1+w)k\Psi + 3\mathcal{H}(\xi_1 r + \xi_2)U_d. \end{aligned} \quad (6)$$

Primes denote derivation with respect to the conformal time, $\mathcal{H} \equiv a'/a$ and $U_\lambda \equiv (1 + w_\lambda)V_\lambda$. $D_\lambda \equiv \delta_\lambda - \frac{\rho'_\lambda}{\rho_\lambda \mathcal{H}}\Phi$ is the gauge invariant density contrast and C_e^2, C_a^2 are the effective and adiabatic sound speed, respectively. In the Newtonian gauge, Ψ, Φ coincide with the gravitational potential ψ, ϕ and V_λ with the peculiar velocity v_λ [61]. Eqs. (3-6) coupled with those describing the evolution of the other energy density perturbations [62], allow us to compute the evolution of the matter gravitational potentials and the peculiar velocity of baryons, and to determine the effect of the DM-DE interaction on the CMB power spectrum.

III. THE INTEGRATED SACHS-WOLFE EFFECT AS A PROBE OF DM-DE INTERACTIONS

Let us consider the effect of the interaction in the late-time ISW effect. As indicated in the introduction, the interaction changes the evolution of the gravitational field, which will result in differences in the growth of density perturbations compared with the concordance cosmological model. The different time evolution of the gravitational potential generates different ISW contributions to the CMB temperature anisotropies and, if measured, it could be used to constrain the interaction.

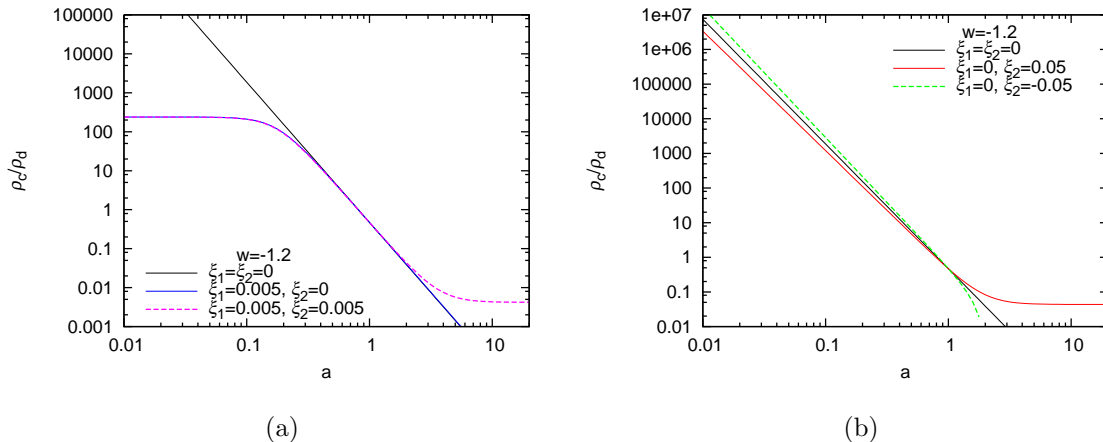


FIG. 1: The evolution of the DM-DE energy density ratio $r \equiv \rho_c/\rho_d$ in a model with an interaction $Q_c = 3H(\xi_1\rho_c + \xi_2\rho_d)$, for different coupling constants.

The ISW effect [64] is the source of temperature anisotropies at early and late times [65]. The latter can be separated from other CMB anisotropies by cross-correlating with templates of projected galaxy density [66] and, therefore, we shall focus on the late-time ISW effect here. The ISW effect can be simply expressed in terms of integration of time-evolution of gravitational potential along the line-of-sight [64],

$$\Delta_\ell^{ISW} = \int_{\tau_i}^{\tau_0} d\tau j_\ell(k[\tau_0 - \tau])e^{-\kappa(\tau)}(\Psi' - \Phi'), \quad (7)$$

where j_ℓ is the spherical Bessel function and κ denotes the optical depth due to Thompson scattering. The time evolution of the gravitational potentials can be described using Einstein's equations

$$\Psi' - \Phi' = 2\mathcal{H}[\Phi + \mathcal{T}] + 8\pi G a^2 \sum_i U_i \rho_i / k - \mathcal{T}', \quad (8)$$

$$\Phi' = -\mathcal{H}\Phi - \mathcal{H}\mathcal{T} - 4\pi G a^2 \sum_i U_i \rho_i / k \quad (9)$$

where

$$\mathcal{T} = \frac{8\pi G a^2}{k^2} (p_\gamma \Pi_\gamma + p_\nu \Pi_\nu). \quad (10)$$

In this expression Π is the anisotropic stress of the relativistic fluid components, that is negligible after matter domination. In this limit, $\Phi = -\Psi$. The photon frequency is shifted on the path to the observer due to time varying gravitational potentials. At low redshifts, the contribution is largest at large angular scales.

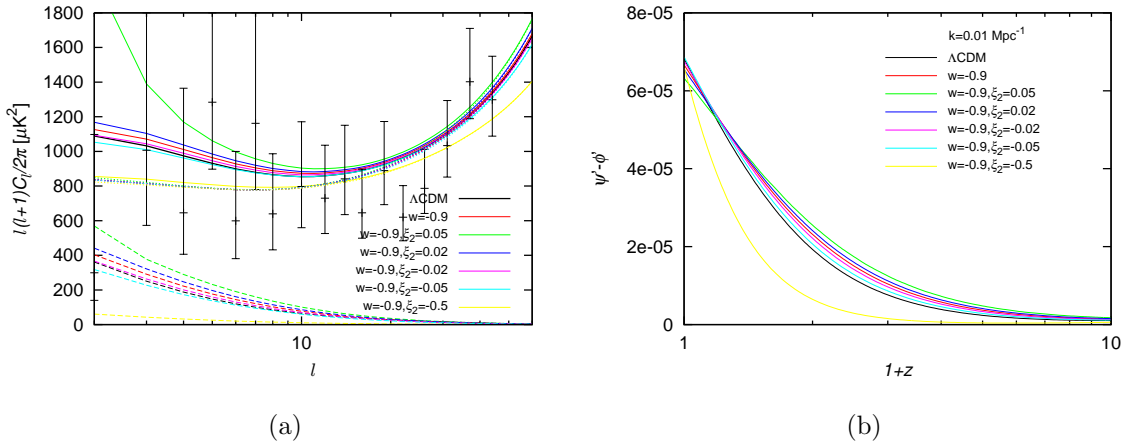


FIG. 2: (a) Solid lines represent the radiation power spectrum of the CMB at large scales for the Λ CDM model and the phenomenological DM-DE interacting model with different couplings; the data and error bars were taken from *Planck* 2013 first data release [63]. Dashed lines display late ISW effect component of the same models. Finally, the dotted lines represent the early ISW effect and SW effect of the same models which are degenerated for the coupling proportional to the energy density of DE. (b) Time derivative of the gravitational potential at lower redshifts, corresponding to a perturbation of wavenumber $k = 0.01\text{Mpc}^{-1}$.

We solve the evolution equations numerically and compute the power spectrum of CMB temperature anisotropies using a version of the Boltzmann code *CMBEASY* [67] publically available, modified according to our model. In Figs. 2, 3, 4, we plot the total radiation power spectrum (solid lines), the ISW component (dashed lines), the SW+early ISW contribution (dotted lines) and the time evolution of the gravitational potentials. In Figs. 2,3 the interaction is proportional to the DE ($\xi_1 = 0$) and the EoS corresponds to quintessence ($w > -1$) and phantom ($w < -1$), respectively. In Fig. 4a the interaction is proportional to the DM ($\xi_2 = 0$) and $w < -1$ since only in this case the growth of matter and dark energy density perturbations does not diverge. In Fig. 4b we show the interaction proportional to the energy density of the dark sector with $\xi_1 = \xi_2 = \xi$ and $w < -1$.

In Fig. 2 we have $\xi_2 > 0$ and the energy is transferred from DE to DM. A positive coupling gives larger fraction of DE in the past than in the concordance model, so that the gravitational potential evolves faster, giving rise to the enhancement of the ISW effect.

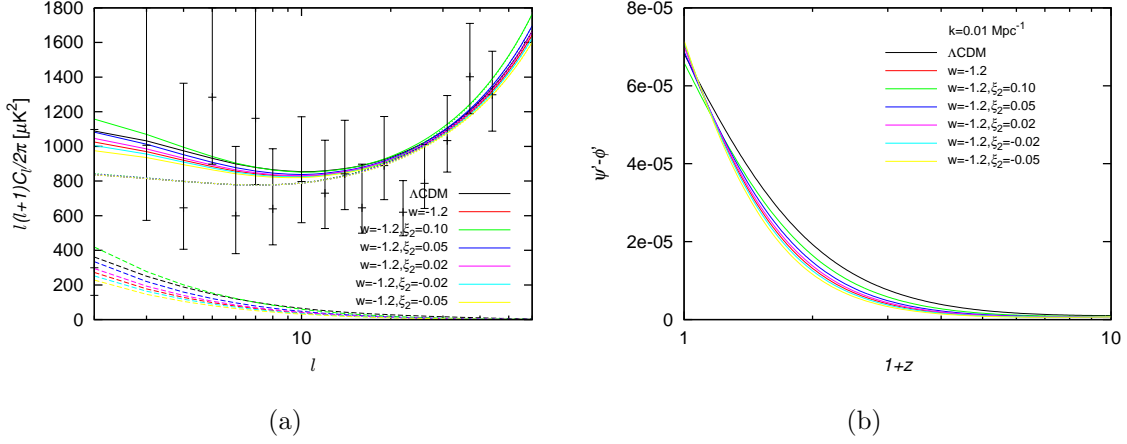


FIG. 3: Same as Fig. 2 but for $w < -1$.

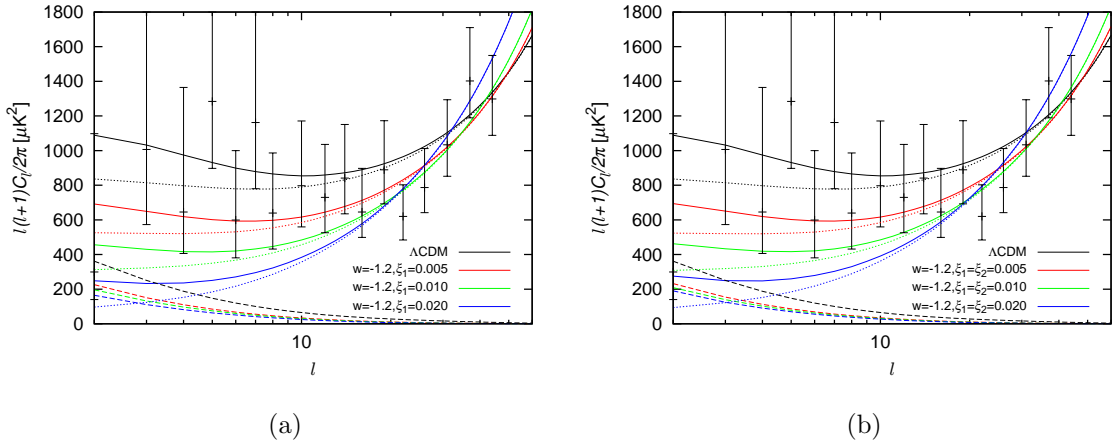


FIG. 4: Radiation power spectra (solid lines), late ISW contribution (dashed lines) and SW+early ISW contributions (dotted lines). In (a) $\xi_1 > 0$ and $\xi_2 = 0$ and in (b)

$\xi_1 = \xi_2 = \xi > 0$.

When the coupling is negative, $\xi_2 < 0$, we have the opposite behavior: the fraction of DE is smaller in the past, slowing the evolution of the gravitational potential and suppressing the ISW effect. In Fig. 3a and Fig. 3b, with parameters $\xi_1 = 0$, $\xi_2 > 0$ and $w < -1$, we find similar behavior. Comparing Fig. 2a and Fig. 3a for the same value of ξ_2 , the ISW is smaller when $w < -1$ than when $w > -1$. In Fig. 4a we plot the results for $\xi_2 = 0$, $w < -1$. In this case, increasing the coupling decreases the ISW effect. Fig. 4b shows the ISW effect in models where the interaction is proportional to the total energy density of the dark sector, which exhibits similar properties than the models of Fig. 4a. Comparison of Fig. 4a and

Fig. 4b shows that the effect of the DE is small compared to that of the DM. As indicated in Sec. 2, since at early times the DM density is much larger than that of the DE, including the DE density in the interaction kernel does not change the evolution significantly. In general, when the fraction of DE in the past increases, the gravitational potential evolves faster, giving rise to a larger ISW effect. This is similar to what happens in the Λ CDM model, when the fraction of Ω_Λ increases.

Together with the late-time ISW effects, there are early ISW anisotropies, generated since the redshift of matter-radiation equality until well after recombination [65] and the Sachs-Wolfe(SW) effect generated on the last scattering surface at large scales. When the interaction is proportional to the DE energy density, the early ISW and the SW effect is little affected since the fraction of DE at high redshifts is small. This can be seen in Fig. 2a and 3a. The dotted lines include the SW and early ISW effects are degenerated and very insensitive to an interaction that is proportional to the DE density. When the interaction is proportional to the DM density, the effect of the interaction in the early ISW and SW anisotropies is larger since the DM is the dominant energy density component after matter-radiation equality. This effect can be seen analyzing the dotted lines in Figs. 4a and 4b. These figures show that the combined SW and early ISW power spectra is more sensitive to the interaction than the late time ISW effect, represented by dashed lines.

To summarize, the results presented in Figs. 2,3,4 indicate that the behavior of the ISW anisotropies is very sensitive to small changes in the strength of the interaction. The SW and early ISW effect components of the CMB temperature anisotropies can not be separated from other contributions. We can probe the effect of the interaction by analyzing how the full CMB power spectrum changes and comparing it with observations. However, cross-correlating CMB maps with templates of projected density of galaxies can separate the contribution of the time variation of the potentials to the late-time ISW effect [66]. Unfortunately, due to cosmic variance the statistical power of the ISW effect to constrain the DM-DE interaction is weak [51]. Nevertheless, the interaction does not only change the time evolution of the gravitational potentials but it also changes the amplitude of potentials [47]. Since the gravitational potential affects the peculiar motions of all particles the interaction, in turn, will modulate peculiar velocities of baryons and their effect on the CMB temperature anisotropies and both effects can be measured as we will see in the next two sections.

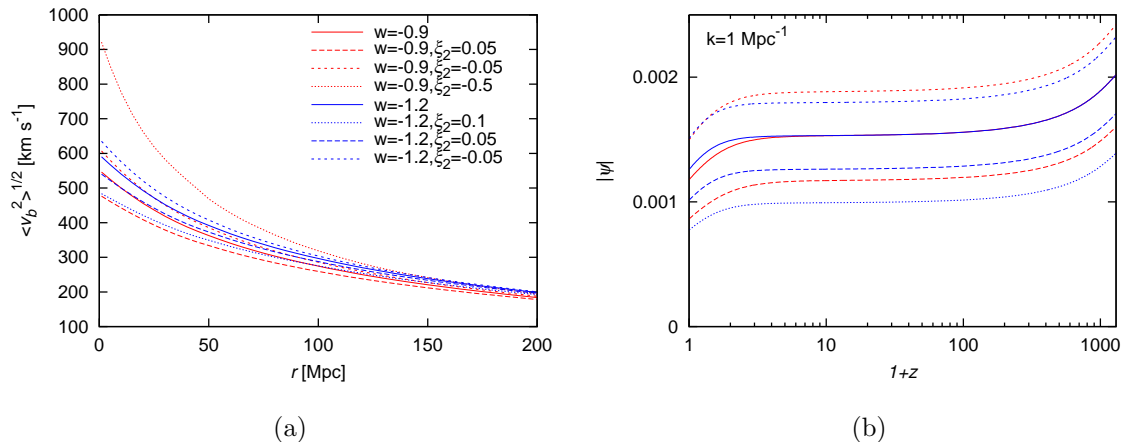


FIG. 5: (a) Root mean square baryon velocity dispersion averaged on a sphere of radius r *vs.* the size of the sphere, for an interaction kernel proportional to DE density. (b) Time evolution of the gravitational potential for a wavenumber $k = 1 \text{ Mpc}^{-1}$. The curves in both panels follow the same convention.

IV. PROBING THE INTERACTION WITH PECULIAR VELOCITIES.

In the standard Λ CDM cosmology, the difference between the velocities of baryon and DM can be neglected at low redshift since baryons trace DM to high accuracy in the linear regime. In the presence of DM-DE interactions, baryons do not trace the DM distribution as perfectly due to the inertial drag effect of DE on DM. The peculiar velocity of baryons is also affected through the influence of the interaction on the curvature perturbation. Thus, it is possible to extract information of the coupling from velocity measurements.

In linear perturbation theory, the evolution equation for the velocity of baryons in Fourier space reads [48]:

$$v_b' = -\mathcal{H}v_b + k\Psi, \quad (11)$$

where the subscript b refers to baryon. This equation shows that baryons are accelerated when falling into the gravitational potential wells. Although the interaction does not appear explicitly in Eq. (11), it affects the evolution of baryon peculiar velocities through the gravitational potential Ψ . Using Einstein's equations, we obtain [24]

$$\Psi = -\Phi = -\frac{4\pi G a^2 \sum_i \rho_i (D_g^i - \rho_i' U_i / (1 + w_i) \rho_i k)}{k^2 - 4\pi G a^2 \sum_i \rho_i' / \mathcal{H}}. \quad (12)$$

The sum is over all energy density components. The main contribution to the gravitational

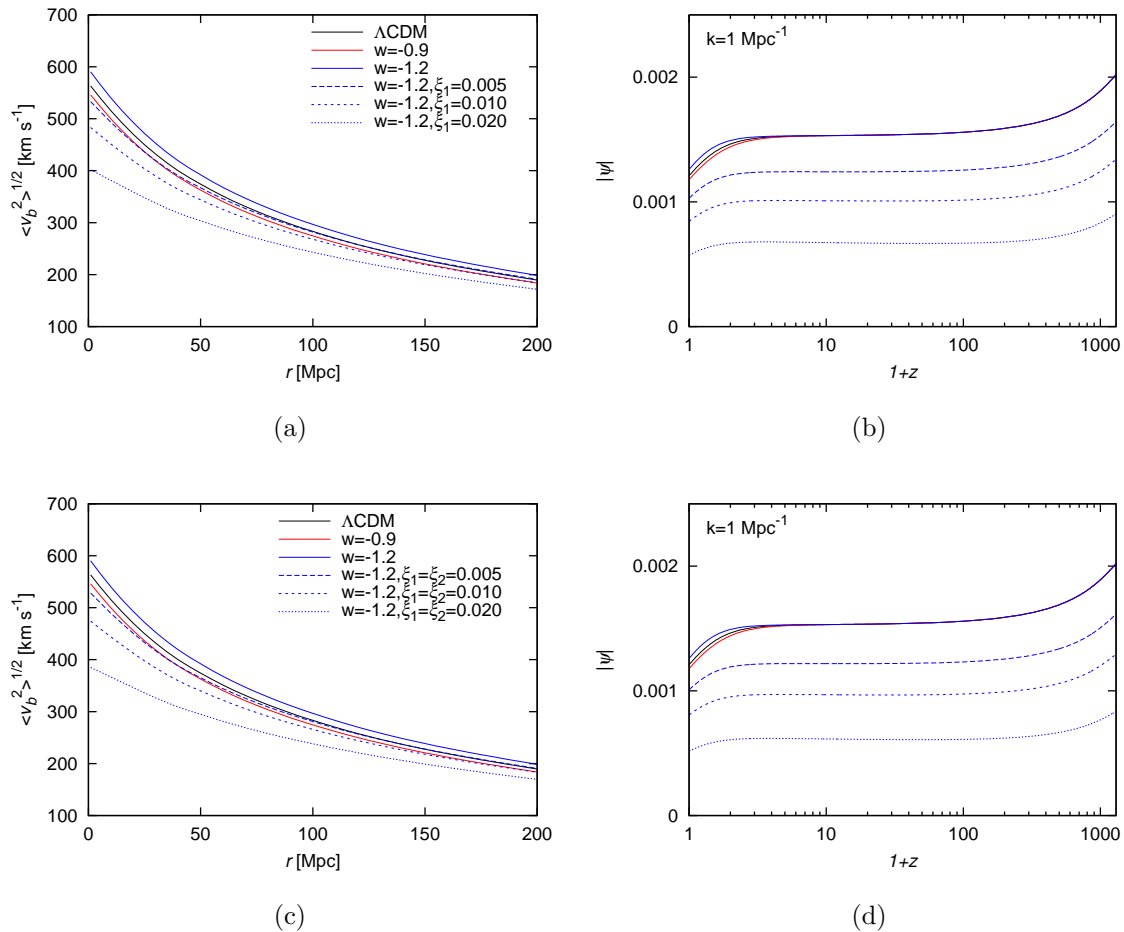


FIG. 6: Same as in Fig. 5 but for: (a) and (b) interaction kernel proportional to the DM; (c) and (d) interaction kernel proportional to the total dark sector with $\xi_1 = \xi_2$. Again, only positive values of ξ_1 and ξ_2 are considered.

potential comes from the DM perturbations which are significantly altered by the interaction. The effect of the interaction within the dark sector is propagated to other components by the gravitational potential and, in particular, it changes the peculiar velocity of baryons.

To compare with observations we compute the root mean square velocity dispersion of the baryon velocity field, smoothed on a sphere of radius r , defined as

$$\langle v_b^2 \rangle = \int d^3k W_r^2(k) P_v(k), \quad (13)$$

where $W_r(k)$ is a top hat window function of radius r and $P_v(k)$ is the power spectrum of the baryon velocity field v_b . The magnitude $\langle v_b^2 \rangle^{1/2}$ represents the mean velocity of the matter within a sphere of radius r with respect to the mean matter distribution, usually known as

bulk flow. For comparison, we also compute the same magnitude for the Λ CDM model.

Our results are presented in Figs. 5 and 6. In the left panels we show the rms velocity dispersion for spheres of different radii and in the right panels the evolution of gravitational potential for $k = 1.0\text{Mpc}^{-1}$. Lines follow the same convention in both left and right panels. In Fig. 5 the results are given for $\xi_1 = 0$ and in Fig. 6 for $\xi_2 = 0$. These figures show that without interaction, the gravitational potential falls slower with decreasing EoS parameter w at small redshifts. This behavior leads to the suppression of the rms peculiar velocity of baryons for $w > -1$ and its enhancement for $w < -1$ compared with the Λ CDM model ($w = -1$). In interacting models the potential evolves for a longer period than in non-interacting models. If $\xi_1 = 0$, increasing the coupling ξ_2 decreases the amplitude of the gravitational potential and reduces the peculiar velocity compared with the concordance model. For $\xi_2 = 0$, the result is similar since larger ξ_1 gives smaller peculiar velocities. Intuitively, stronger the coupling larger the fraction of DE in the past, reducing the amplitude of the gravitational field and consequently, also the amplitude of the matter peculiar velocity. For a positive coupling, the effect on the peculiar velocities is larger when the coupling is proportional to the DM than to the DE, as it could be expected since the DM energy density is larger than that of the DE during most of the evolution history of the Universe. In Fig. 6c we show the peculiar velocity when the interaction is proportional to the total energy density of the dark sector. Again, the behavior is very similar to the case with interaction proportional to the DM energy only. The greatest variation with respect to the concordance model occurs when $\xi_2 < 0$ and $w < -1$, when the peculiar velocity could be larger by a factor of two.

Observationally it is difficult to measure peculiar velocities on scales above $50h^{-1}\text{Mpc}$ using galaxies. In [68] it was proposed to use clusters as tracers of the velocity field since the kSZ effect provides their peculiar velocity with respect to the matter rest frame. The results of [53–55] suggest that the local CMB dipole is not associated with our peculiar motion but is intrinsic to the Last Scattering Surface. If so, those results would not constrain any possible interaction on the dark sector. A more direct probe would be the measurement of the pair-wise velocity dispersion of clusters [56] since it is related to the matter peculiar velocity. While the results from Atacama Cosmology Telescope (ACT) [56] and *Planck* [52] seem to be consistent with the Λ CDM model, given their large uncertainties they are also compatible with the models considered here. To conclude, while at present the data does

not have the statistical power to constrain the interaction, the peculiar velocity field could become an important test of the interaction with future data sets of higher resolution and lower noise.

V. THE POWER SPECTRUM OF KINETIC SUNYAEV-ZEL'DOVICH TEMPERATURE ANISOTROPIES

The interaction changes the matter velocity field at all redshifts, therefore it does not only affect the peculiar velocity field on the local Universe, traced by galaxies or clusters, but also the velocity field since recombination. Therefore, temperature anisotropies induced by the ionized gas in unresolved sources up to the present will generate a different pattern of kSZ temperature anisotropies on the CMB and the power spectrum of the kSZ effect will be sensitive to any DM-DE interaction.

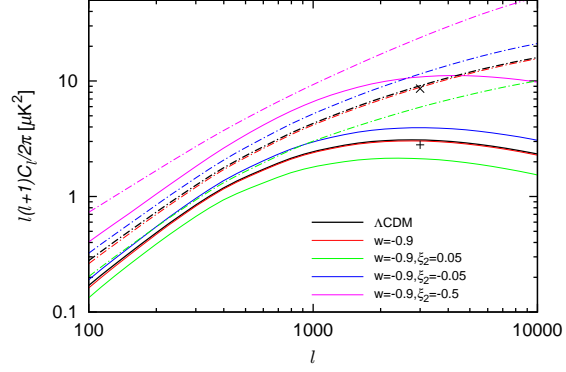
To take into account the contribution of all the ionized gas to the temperature anisotropies of the CMB, we need to compute the effect of all unresolved sources present in the Universe. At redshift $z \lesssim 10$, the reionization of the intergalactic medium will produce free electrons that would share the same motion as the average baryon. CMB photons, re-scattered by this moving plasma, give rise to secondary temperature anisotropies as [69]

$$\frac{\Delta T(\hat{\mathbf{n}})}{T_{\text{CMB}}} = - \int_{t_{\text{re}}}^{t_0} n_e \sigma_T e^{-\kappa} (\mathbf{v} \cdot \hat{\mathbf{n}}) dt, \quad (14)$$

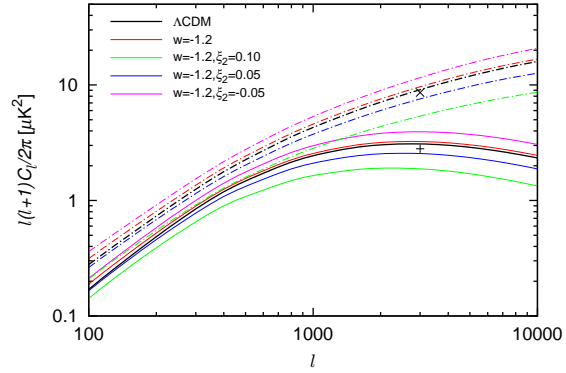
where n_e is the electron density, σ_T is the Thomson cross section and κ is the Thomson optical depth, \mathbf{v} is the peculiar velocity of the electrons; the integral is along the line of sight (l.o.s.) out to the reionization epoch and $\hat{\mathbf{n}}$ is the unit vector along the l.o.s. Using the comoving distance x and neglecting any interaction of electrons with other particles, we can write $n_e(x, z) = \chi_e \bar{n}_e(0) a^{-3} [1 + \delta_e(x, z)]$, where $\bar{n}_e(0)$ is the mean electron number density at present and χ_e is the ionization fraction. Within this approximation

$$\frac{\Delta T(\hat{\mathbf{n}})}{T_{\text{CMB}}} = \bar{n}_e(0) \sigma_T \int a^{-2} \chi_e e^{-\kappa} (\mathbf{p} \cdot \hat{\mathbf{n}}) dx, \quad (15)$$

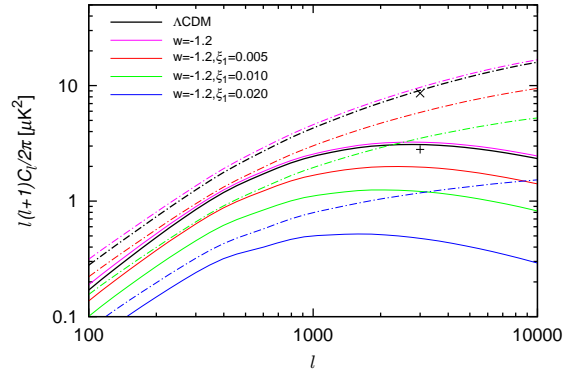
where we have defined the peculiar momentum $\mathbf{p} \equiv (1 + \delta_e) \mathbf{v}$; \mathbf{p} can be decomposed into a gradient component \mathbf{p}_E and a curl component \mathbf{p}_B . The gradient term cancels out when integrating along the l.o.s. and has no contribution to the kSZ effect. The net effect is only due to the curl part of the peculiar momentum [70, 71].



(a)



(b)



(c)

FIG. 7: Radiation power spectrum of the CMB temperature anisotropies generated by the kinetic Sunyaev-Zel'dovich effect for different interaction kernels: (a) $\xi_1 = 0$, $w > -1$; (b) $\xi_1 = 0$, $w < -1$ and (c) $\xi_2 = 0$, $w < -1$. Solid lines correspond to the linear power spectra and dot-dashed lines to non-linear power spectra.

Since the kSZ effect induces temperature fluctuations at small angular scales, the correlation function of the temperature anisotropies between two positions in the sky separated by an angle θ can be calculated using Limber approximation; then

$$\begin{aligned} w(\theta) &\approx (n_e(0)\sigma_T)^2 \cos(\theta) \int_0^{x_{\text{re}}} dx (a^{-2}\chi_e)^2 \exp(-2\kappa(z)) \int_{-\infty}^{\infty} \frac{1}{2} \xi_B(\sqrt{x^2\theta^2 + y^2}) dy \\ &\approx (n_e(0)\sigma_T)^2 \int_0^{x_{\text{re}}} dx (a^{-2}\chi_e)^2 \exp(-2\kappa(z)) \int_{-\infty}^{\infty} \frac{1}{2} \xi_B(\sqrt{x^2\theta^2 + y^2}) dy, \end{aligned} \quad (16)$$

where ξ_B is the correlation function of \mathbf{p}_B . In eq. (16) we have used the identity $\langle |\mathbf{p}_B(\mathbf{k}) \cdot \hat{\mathbf{n}}|^2 \rangle = P_B^2(k)/2$, where $P_B(k)$ is the power spectrum of $\mathbf{p}_B(\mathbf{k})$. The contribution of the kSZ effect to CMB temperature anisotropies now reads

$$C_l^{kSZ} = \frac{16\pi^2}{(2l+1)^3} (\bar{n}_e(0)\sigma_T)^2 \int_0^{z_{\text{re}}} (1+z)^4 \chi_e^2 \frac{1}{2} \Delta_B^2(k, z)|_{k=l/x} e^{-\kappa} x(z) \frac{dx(z)}{dz} dz, \quad (17)$$

where $\Delta_B^2(k, z) = \frac{k^3}{2\pi^2} P_B(k, z)$.

Let us now analyze the contributions to the solenoidal part of the electron velocity field. Since $\nabla \times \mathbf{p} = (1 + \delta_e)\nabla \times \mathbf{v} + \nabla \delta_e \times \mathbf{v}$, there are only two possible contributions: from the rotational mode of \mathbf{v} or from the correlation between the density and the velocity fields. In the linear regime, only the irrotational component of the velocity fields couples to gravity, so the first contribution is zero; the kSZ effect is due to the correlation between the density gradient and the velocity. In Fourier space,

$$\begin{aligned} P_B(k) &= \langle \mathbf{p}_B^*(\mathbf{k}) \mathbf{p}_B(\tilde{\mathbf{k}}) \rangle = \int \frac{d^3\mathbf{k}'}{(2\pi)^3} \int \frac{d^3\tilde{\mathbf{k}}'}{(2\pi)^3} \langle \delta_e^*(\mathbf{k} - \mathbf{k}') \delta_e(\tilde{\mathbf{k}} - \tilde{\mathbf{k}}') \mathbf{v}^*(\mathbf{k}') \mathbf{v}(\tilde{\mathbf{k}}') \rangle \\ &\quad \times |\mathbf{k}'| |\tilde{\mathbf{k}}'| \beta(\mathbf{k}, \mathbf{k}') \beta(\tilde{\mathbf{k}}, \tilde{\mathbf{k}}'), \end{aligned} \quad (18)$$

where $\beta(\mathbf{k}, \mathbf{k}') = [\mathbf{k}' - \mathbf{k}(\mathbf{k} \cdot \mathbf{k}')/k^2]/k'^2$. Notice that in (18), \mathbf{k}' , $\tilde{\mathbf{k}}'$ and $\mathbf{k} - \mathbf{k}'$, $\tilde{\mathbf{k}} - \tilde{\mathbf{k}}'$ can be interchanged.

In the linear perturbation theory, using the subhorizon approximation, the relation between peculiar velocities and density perturbations are given by

$$v = -\delta'_e/k = -aHf_e(a)\delta_e/k, \quad (19)$$

where $f_e = \frac{d \ln \delta_e}{d \ln a}$ is the growth factor for electron density perturbations, which at this order in perturbation theory is the same as the baryonic matter growth factor, but is different from that of DM in the presence of DM-DE interaction. By defining $D_e(z) \equiv \delta_e(z)/\delta_e(0)$,

we can rewrite $aHf_e = a\dot{D}_e/D_e$ and

$$P_B(k, z) = \frac{a^2}{2} \int \frac{d^3\mathbf{k}'}{(2\pi)^3} \left(\frac{\dot{D}_e}{D_e} \right)^2 P(k', z) P(k - k', z) \times [W_g(k - k')\beta(\mathbf{k}, \mathbf{k}') + W_g(k')\beta(\mathbf{k}, \mathbf{k} - \mathbf{k}')]^2, \quad (20)$$

where $P(k)$ is the baryon power spectrum, $W_g(k)$ is the transfer function which takes into account the suppression of baryon density fluctuations at small scales due to physical processes [72]. For simplicity, we have set it to unity in our numerical calculations.

Eqs. (17,20) give the contributions of the ionized gas to the temperature anisotropies of the CMB. Let us remark that eq. (17) depends implicitly on the DM-DE interaction. Since the fraction of ionized gas evolves as

$$\delta_e'' + \frac{a'}{a}\delta_e' + 3\phi'' + 3H\phi' + k^2\psi = 0. \quad (21)$$

In the small scale approximation the time variation of the potential can be neglected with respect to their spatial gradients. Using Poisson equation we can write

$$\delta_e'' + \frac{a'}{a}\delta_e' - 4\pi G a^2(\rho_b\delta_b + \rho_c\delta_c + \rho_d\delta_d) = 0, \quad (22)$$

Since DM and DE density perturbations depend on the interaction (see eqs. 3-6), the time evolution of background and perturbed magnitudes ρ_c , ρ_d , δ_c and δ_d will be modified, changing the evolution of the gravitational potential ψ . The density perturbation of free electrons, δ_e , will also be modified. Due to the interaction, the evolution of both the gravitational potential and density perturbations are scale-dependent, which is different from that in the Λ CDM cosmology, where all sub-horizon perturbations grow at the same rate. Thus, a scale dependent behavior could be very useful to constrain observationally any possible interaction.

The non-linear evolution of matter density perturbations enhances the kSZ effect. Following [73–75], this contribution changes the expression of (20) to

$$P_B(k, z) = \frac{a^2}{2} \int \frac{d^3\mathbf{k}'}{(2\pi)^3} \left(\frac{\dot{D}_e}{D_e} \right)^2 P(k', z) P(k - k', z) \times [W_g(k - k')T_{NL}(k - k')\beta(\mathbf{k}, \mathbf{k}') + W_g(k')T_{NL}(k')\beta(\mathbf{k}, \mathbf{k} - \mathbf{k}')]^2, \quad (23)$$

where we have defined the non-linear power spectrum as $P^{NL}(k) \equiv P(k)T_{NL}^2(k)$. The non-linear correction affects the density and not the velocity field [73, 74], as could be expected

since matter density perturbations can be highly non-linear while the velocity field is still in the linear regime [76]. To include the non-linear correction we need to specify the non-linear power spectrum of baryon density perturbations which is usually done by using adequate fits to numerical simulations. Such simulations had not been carried out for interacting DM and DE models so for this type of models we can only guess what the non-linear power spectrum could be, making it difficult to give a reliable estimate of the non-linear contribution. One further complication is that on small scales the dynamics of baryons and pressureless DM particles is very different. While non-linear corrections can enhance the amplitude of the kSZ effect by a factor 2-4 in the range $\ell = 3 \times 10^3 \sim 10^4$, physical processes on the baryon component such as shock heating and dissipation can reduce the change to only 0.3-2, in the same range of multipoles [75].

An estimate of the non-linear contribution can be given if we assume that the nonlinear evolution of baryon density perturbations is weakly dependent on the effect of the interaction. Thus, we can construct the non-linear correction to the linear power spectrum in the interacting model like in the concordance model: $P^{NL}(k) = P(k)T_{NL}^2(k)$, where $P(k)$ is the baryon linear density power spectrum, and the transfer function $T_{NL}(k)$ identical to the concordance model. In the following numerical calculations, we employ the halofit model developed in [77] and revised in [78] to estimate the non-linear corrections.

In Fig. 7 we represent the linear (solid lines) and non-linear (dot-dashed lines) kSZ power spectrum. The three plots correspond to our fiducial models: (a) $\xi_1 = 0$, $w > -1$; (b) $\xi_1 = 0$, $w < -1$; and (c) $\xi_2 = 0$, $w < -1$. The curves corresponding to the non-linear kSZ effect are essentially upper limits since we do not take into account the small scale smoothing of the baryon density perturbations due to gas pressure. Fig. 7 shows that in models with no interaction the kSZ power spectrum is weakly dependent on w . With DM-DE interaction, the amplitude increases with decreasing ξ_2 ; it is smaller than the non-interaction model when $\xi_2 > 0$ and larger when $\xi_2 < 0$. In Fig. 7b the kSZ power spectrum amplitude also increases with decreasing ξ_2 . The same behavior is observed in Fig. 7c with the exception that the spectrum is always below models without interaction since we have restricted our study to the case $\xi_1 > 0$. The results presented in Fig. 7 follow those of Figs. 5, 6 that also showed that positive couplings suppress the amplitude of the peculiar velocities, resulting in a smaller kSZ effect. Even though the kSZ spectrum is enhanced by including the non-linear effect, the scaling behavior with the coupling parameter is the same as in the linear case.

In Fig. 7, we include two upper limits to the amplitude of the kSZ power spectrum at the 95% confidence level. The cross, located at $8.6\mu K^2$ was derived from the ACT data at $\ell = 3000$ [79]. The plus is the $2.8\mu K^2$ upper limit at $\ell = 3000$ derived from the South Pole Telescope (SPT) data [80]. These upper limits depend on the reionization history and on the modeling of Cosmic Infrared Background and thermal Sunyaev-Zel'dovich contributions. Nevertheless, these results are already in tension with negative coupling in DM-DE interaction and tend to favor positive coupling (see Fig. 7). A number of complexities could change the constraints. On the one hand, the kSZ effect from patchy reionization is expected to be comparable with that from the homogeneous part. Hence the 95% upper limit on the homogeneous kSZ effect would be significantly smaller than the quoted figures from ACT and SPT. On the other, we did not include effect of gas pressure in our calculation that could potentially reduce the amplitude of the kSZ spectrum. Despite these uncertainties, taken the data at face value, the kSZ observations favor a positive coupling between DM-DE interaction. This result is encouraging, since it is consistent with our previous constraints from the CMB [36, 48] and galaxy clusters [45, 46]. Such positive coupling means that the energy flows from DE to DM, as required to alleviate the coincidence problem and to satisfy the second law of thermodynamics [27]. A positive coupling is also very reassuring in the light of the coincidence problem. As Fig. 1 shows, the background evolution contains a long period in the expansion of the Universe where DM and DE densities are comparable to each other.

VI. CONCLUSIONS

In this paper we have studied the effect of the DM-DE interaction in the gravitational field and matter peculiar velocities. We have analyzed how three different observables, the ISW effect, the matter peculiar velocity and the CMB temperature anisotropies induced by the kSZ effect, are sensitive to the interaction. The latter two effects have been considered in this paper for the first time. We have shown that the amplitude of the kSZ effect, like the ISW effect, is sensitive to the amplitude and sign of the interaction. Although both effects are related to the gravitational potential, the late-time ISW effect is determined by the time-evolving gravitational potential, while peculiar velocities and the kSZ effect depend on the accelerations generated by the potentials themselves. Both tests are complementary

with each other since they reflect physical processes in the CMB that operate at different scales. For instance, the ISW effect probes the effect of the interaction during the period of accelerated expansion since the potentials are roughly constant during the matter dominated regime while the kSZ effect receives contribution since reionization at $z \lesssim 10$. Then, the time evolution of the gravitational potential that generate the ISW effect contributes to CMB anisotropies mostly at large angular scales while the kSZ effect, that depends on the projection of the peculiar velocity field along the line of sight, contributes preferentially at $\ell > 10^3$. Figs. 5, 6 show that even if the evolution of the gravitational potential changes little with time, the amplitude of the gravitational potential can vary significantly due to a DM-DE interaction. The strong dependence of δ_e and v , which contributes to the rotational part of the peculiar momentum, on the gravitational potential suggests that the kSZ effect is more sensitive to the interaction than the ISW effect. Furthermore, since the kSZ effect is dominant at small angular scales, it is less affected by cosmic variance. These secondary anisotropies could become a powerful tool to discriminate models with interaction.

By using the upper limits on the kSZ effect from ACT and SPT, we have seen that these data favors an interaction between DE and DM with a positive coupling, which is consistent with the previous CMB constraints [36, 48] and the galaxy cluster scale tests [45, 46]. This positive coupling means that there is energy flow from DE to DM, which can alleviate the coincidence problem. Further details of the kSZ spectrum could be detected with the next generation of CMB observations with high resolution, like Gismo¹. If this forthcoming experiment achieves the expected sensitivity, it could provide the first detection of the interaction within the dark sector.

Alternatively, the peculiar velocity of resolved clusters can be used to trace the velocity field at different scales [53–57]. Models with interaction could give peculiar velocities with an amplitude about a factor of 2 larger or 5 smaller than the Λ CDM prediction. Combining this observable with the ISW and kSZ power spectrum can provide a measurement of the interaction or upper limits on the amplitude of the coupling stronger than those currently available.

¹ <http://www.iram.es/IRAMES/mainWiki/GoddardIramSuperconductingTwoMillimeterCamera>

Acknowledgments

This work was partially supported by the National Natural Science Foundation of China and project FIS2012-30926 from the spanish Ministerio de Ciencia e Innovación. We would like to acknowledge helpful discussions with E. Abdalla and D. Pavon.

-
- [1] S. Perlmutter, G. Aldering, M. D. Valle, S. Deustua, R. S. Ellis, S. Fabbro, A. Fruchter, G. Goldhaber, A. Goobar, D. E. Groom, et al., *Nature* **391**, 51 (1998).
 - [2] A. G. Riess, A. V. Filippenko, P. Challis, A. Clocchiattia, A. Diercks, P. M. Garnavich, R. L. Gilliland, C. J. Hogan, S. Jha, R. P. Kirshner, et al., *Astron.J.* **116**, 1009 (1998).
 - [3] S. Perlmutter, G. Aldering, G. Goldhaber, R. A. Knop, P. Nugent, P. G. Castro, S. Deustua, S. Fabbro, A. Goobar, D. E. Groom, et al., *Astrophys.J.* **517**, 565 (1999).
 - [4] J. L. Tonry, B. P. Schmidt, B. Barris, P. Candia, P. Challis, A. Clocchiatti, A. L. Coil, A. V. Filippenko, P. Garnavich, C. Hogan, et al., *Astrophys.J.* **594**, 1 (2003).
 - [5] A. G. Riess, L.-G. Strolger, J. Tonry, S. Casertano, H. C. Ferguson, B. Mobasher, P. Challis, A. V. Filippenko, S. Jha, W. Li, et al., *Astrophys.J.* **607**, 665 (2004).
 - [6] P. Astier, J. Guy, N. Regnault, R. Pain, E. Aubourg, D. Balam, S. Basa, R. G. Carlberg, S. Fabbro, D. Fouchez, et al., *Astron.Astrophys.* **447**, 31 (2006).
 - [7] A. G. Riess, L.-G. Strolger, S. Casertano, H. C. Ferguson, B. Mobasher, B. Gold, P. J. Challis, A. V. Filippenko, S. Jha, W. Li, et al., *Astrophys.J.* **659**, 98 (2007).
 - [8] G. Hinshaw, D. Larson, E. Komatsu, D. N. Spergel, C. L. Bennett, J. Dunkley, M. R.olta, M. Halpern, R. S. Hill, N. Odegard, et al., *ApJS* in press (2012).
 - [9] PlanckCollaboration, Submitted to *A&A* (2013).
 - [10] S. Micheletti, E. Abdalla, and B. Wang, *Phys.Rev.D* **79**, 123506 (2009).
 - [11] S. M. R. Micheletti, *JCAP* **1005**, 009 (2009).
 - [12] L. Amendola, *Phys.Rev.D* **62**, 043511 (2000).
 - [13] L. Amendola and C. Quercellini, *Phys.Rev.D* **68**, 023514 (2003).
 - [14] L. Amendola, S. Tsujikawa, and M. Sami, *Phys.Lett. B* **632**, 155 (2006).
 - [15] D. Pavon and W. Zimdahl, *Phys.Lett.B* **628**, 206 (2005).
 - [16] S. del Campo, R. Herrera, and D. Pavon, *Phys.Rev.D* **78**, 021302 (2008).

- [17] C. G. Boehmer, G. Caldera-Cabral, R. Lazkoz, and R. Maartens, *Phys.Rev.D* **78**, 023505 (2008).
- [18] S. Chen, B. Wang, and J. Jing, *Phys.Rev.D* **78**, 123503 (2008).
- [19] B. Wang, Y. Gong, and E. Abdalla, *Physics Letters B* **624**, 141 (2005).
- [20] S. Das, P. S. Corasaniti, and J. Khoury, *Phys. Rev. D* **73**, 083509 (2006).
- [21] G. a. n. Olivares, F. Atrio-Barandela, and D. Pavón, *Phys. Rev. D* **71**, 063523 (2005).
- [22] G. Olivares, F. Atrio-Barandela, and D. Pavón, *Phys. Rev. D* **77**, 063513 (2008).
- [23] J. Valiviita, E. Majerotto, and R. Maartens, *JCAP* **07**, 020 (2008).
- [24] J.-H. He, B. Wang, and E. Abdalla, *Phys.Lett.B* **671**, 139 (2008).
- [25] P. S. Corasaniti, *Phys.Rev.D* **78**, 083538 (2008).
- [26] B. M. Jackson, A. Taylor, and A. Berera, *Phys. Rev. D* **79**, 043526 (2009).
- [27] D. Pavon and B. Wang, *Gen.Rel.Grav.* **41**, 1 (2007).
- [28] B. Wang, C.-Y. Lin, D. Pavon, and E. Abdalla, *Phys.Lett.B* **662**, 1 (2007).
- [29] B. Wang, J. Zang, C.-Y. Lin, E. Abdalla, and S. Micheletti, *Nucl.Phys.B* **778**, 69 (2007).
- [30] F. Simpson, B. M. Jackson, and J. A. Peacock, *MNRAS* **411**, 1053 (2011).
- [31] W. Zimdahl, *Int.J.Mod.Phys. D* **14**, 2319 (2005).
- [32] Z.-K. Guo, N. Ohta, and S. Tsujikawa, *Phys.Rev.D* **76**, 023508 (2007).
- [33] C. Feng, B. Wang, E. Abdalla, and R.-K. Su, *Phys.Lett.B* **665**, 111 (2008).
- [34] J. Valiviita, R. Maartens, and E. Majerotto, *Mon. Not. R. Astron. Soc.* **402**, 2355 (2009).
- [35] J.-Q. Xia, *Phys.Rev.D* **80**, 103514 (2009).
- [36] J.-H. He, B. Wang, and P. Zhang, *Phys.Rev.D* **80**, 063530 (2009).
- [37] M. Martinelli, L. L. Honorez, A. Melchiorri, and O. Mena, *Phys.Rev.D* **81**, 103534 (2010).
- [38] L. L. Honorez, B. A. Reid, O. Mena, L. Verde, and R. Jimenez, *JCAP* **09**, 029 (2010).
- [39] J.-H. He and B. Wang, *JCAP* **06**, 010 (2008).
- [40] J.-H. He, B. Wang, and Y. P. Jing, *JCAP* **07**, 030 (2009).
- [41] G. Caldera-Cabral, R. Maartens, and B. M. Schaefer, *JCAP* **07**, 027 (2009).
- [42] J.-H. He, B. Wang, E. Abdalla, and D. Pavon, *JCAP* **12**, 022 (2010).
- [43] O. Bertolami, F. G. Pedro, and M. L. Delliou, *Phys.Lett.B* **654**, 165 (2007).
- [44] O. Bertolami, F. Gil Pedro, and M. Le Delliou, *General Relativity and Gravitation* **41**, 2839 (2009).
- [45] E. Abdalla, L. R. Abramo, L. Sodre, and B. Wang, *Physics Letters B* **673**, 107 (2009).

- [46] E. Abdalla, L. R. Abramo, and J. C. C. de Souza, *Phys. Rev. D* **82**, 023508 (2009).
- [47] G. Olivares, F. Atrio-Barandela, and D. Pavon, *Phys.Rev.D* **74**, 043521 (2006).
- [48] J.-H. He, B. Wang, and E. Abdalla, *Phys.Rev.D* **83**, 063515 (2011).
- [49] X.-D. Xu, J.-H. He, and B. Wang, *Phys.Lett. B* **701**, 513 (2011).
- [50] V. Salvatelli, A. Marchini, L. Lopez-Honorez, and O. Mena (2013).
- [51] G. Olivares, F. Atrio-Barandela, and D. Pavón, *Phys. Rev. D* **77**, 103520 (2008).
- [52] Planck intermediate results. XIII. (2013), arXiv:1303.5090.
- [53] A. Kashlinsky, F. Atrio-Barandela, D. Kocevski, and H. Ebeling, *Astrophys.J.* **686**, L49 (2008).
- [54] A. Kashlinsky, F. Atrio-Barandela, H. Ebeling, A. Edge, and D. Kocevski, *Astrophys.J.* **712**, L81 (2010).
- [55] A. Kashlinsky, F. Atrio-Barandela, and H. Ebeling, *Astrophys.J.* **732**, 1 (2011).
- [56] N. Hand, G. E. Addison, E. Aubourg, N. Battaglia, E. S. Battistelli, D. Bizyaev, J. R. Bond, H. Brewington, J. Brinkmann, B. R. Brown, et al., *Phys. Rev. Lett.* **109**, 041101 (2012).
- [57] T. Mroczkowski, S. Dicker, J. Sayers, E. D. Reese, B. Mason, N. Czakon, C. Romero, A. Young, M. Devlin, S. Golwala, et al., *ApJ* **761**, 47 (2012).
- [58] P. Bull, T. Clifton, and P. G. Ferreira, *Phys. Rev. D* **85**, 024002 (2011).
- [59] R. Genova-Santos, F. Atrio-Barandela, J. Muecket, and J. Klar, *Astrophys.J.* **700**, 447 (2009).
- [60] P. Zhang, *MNRAS Letters*, **407**, L36 (2010).
- [61] H. Kodama and M. Sasaki, *Progress of Theoretical Physics Supplement* **78**, 1 (1984).
- [62] C.-P. Ma and E. Bertschinger, *Astrophys.J.* **455**, 7 (1995).
- [63] Planck 2013 results. XV. (2013), arXiv:1303.5075.
- [64] R. K. Sachs and A. M. Wolfe, *Astrophys. J.* **147**, 73 (1967).
- [65] W. Hu and N. Sugiyama, *Phys. Rev. D* **51**, 2599 (1995).
- [66] R. G. Crittenden and N. Turok, *Phys. Rev. Lett.* **76**, 575 (1996).
- [67] M. Doran, *JCAP* **0506**, 011 (2005).
- [68] A. Kashlinsky and F. Atrio-Barandela, *ApJ* **536**, L67 (2000).
- [69] R. A. Sunyaev and Y. B. Zeldovich, *Comments on Astrophysics and Space Physics* **4**, 173 (1972).
- [70] E. T. Vishniac, *Astrophys.J.* **322**, 597 (1987).
- [71] P. Zhang, U.-L. Pen, and H. Trac, *Mon.Not.Roy.Astron.Soc.* **347**, 1224 (2004).

- [72] L.-Z. Fang, H. Bi, S. Xiang, and G. Boerner, *ApJ* **413**, 477 (1993).
- [73] W. Hu, *Astrophys.J.* **529**, 12 (2000).
- [74] C.-P. Ma and J. N. Fry, *Phys.Rev.Lett.* **88**, 211301 (2002).
- [75] L. D. Shaw, D. H. Rudd, and D. Nagai (2011).
- [76] P. Coles and B. Jones, *MNRAS* **248**, 1 (1991).
- [77] R. E. Smith, J. A. Peacock, A. Jenkins, S. D. M. White, C. S. Frenk, F. R. Pearce, P. A. Thomas, G. Efstathiou, H. M. P. Couchmann, and T. V. Consortium, *Mon.Not.Roy.Astron.Soc.* **341**, 1311 (2003).
- [78] R. Takahashi, M. Sato, T. Nishimichi, A. Taruya, and M. Oguri, *The Astrophysical Journal* **761**, 152 (2012).
- [79] J. L. Sievers, R. A. Hlozek, M. R. Nolta, V. Acquaviva, G. E. Addison, P. A. R. Ade, P. Aguirre, M. Amiri, J. W. Appel, L. F. Barrientos, et al. (2013).
- [80] C. L. Reichardt, L. Shaw, O. Zahn, K. A. Aird, B. A. Benson, L. E. Bleem, J. E. Carlstrom, C. L. Chang, H. M. Cho, T. M. Crawford, et al., *ApJ* **755**, 70 (2012).